Estimating vertical ground reaction forces for rearfoot runners using a minimal IMU setup

For different running speeds and step frequencies

Hazal Usta (Student M-BME)
Master Thesis

Supervisors
dr. J. Reenalda
dr. E.H.F. van Asseldonk
ir. B.L. Scheltinga

Faculty of Science and Technology
Biomedical Engineering

SAMENVATTING

Grondreactiekracht is belangrijke maat om lichaamsbeweging te identificeren. Iemand die staat, loopt of rent genereert een kracht op de grond en als reactie wordt de grondreactiekracht op het lichaam uitgeoefend. De grondreactiekrachten vertegenwoordigen de belasting die op het lichaam werkt en worden daarom vaak bestudeerd bij hardloopactiviteiten. Deze kracht kan tijdens het hardlopen variëren van 2 tot 3 keer het lichaamsgewicht en wordt geassocieerd met hardloopblessures. De grondreactiekracht bestaat uit drie componenten, waarvan de verticale kracht de grootste en belangrijkste component is bij het bestuderen van blessures. De verticale grondreactiekracht bestaat uit eerst een 'impactpiek' en daarna een actieve piek. De eerste piek wordt gegenereerd door de impact die de voet maakt met de grond en de tweede piek is een reactie van de afzetkracht die de voet op de grond uitoefent. Grondreactiekrachten kunnen worden gemeten met behulp van krachtplaten gemonteerd in de vloer of geïnstrumenteerd in loopbanden. Een nadeel van deze methode is dat deze beperkt is tot de laboratoriumomgeving. Grondreactiekrachten kunnen ook worden geschat op basis van andere variabelen. Dit zou gebruikt kunnen worden om buiten het laboratorium de belasting op het lichaam te bepalen. Er zijn verschillende algoritmes ontwikkeld om grondreactiekrachten te schatten op basis van inertiële meetsensoren (IMU's), maar er is nog geen onderzoek gedaan naar het schatten van verschillende snelheden en stapfrequenties voor hardlopers met een haklanding. Het doel van deze studie is om een generiek algoritme te ontwikkelen om de verticale component van de grondreactiekrachten van lopers met een haklanding te schatten, met behulp van een minimaal aantal IMUs.

Acht gezonde, ervaren hardlopers met haklanding (leeftijd: 33,75 ± 10,98 jaar; lengte: 1,77 ± 0,08 cm; massa: 70,46 ± 14,50 kg; geslacht: 5 mannen/3 vrouwen) hebben deelgenomen aan dit onderzoek. Elke deelnemer heeft 90 seconden gerend op drie verschillende snelheden (in willekeurige volgorde 10, 12 en 14 km/u) en drie verschillende stapfrequenties (100%, 110% en 90% van de gewenste stapfrequentie). Metingen zijn uitgevoerd met het MVN Link systeem, waarbij acht sensoren op het lichaam van de deelnemers was bevestigd. Data dat was verzameld met de acht sensoren werd gebruikt om een algoritme te ontwerpen voor het schatten van de verticale grondreactiekracht. Het algoritme is gebaseerd op de tweede wet van Newton en gebruikt de versnellingen van de sensoren in het globale frame. Naast de sensordata werden ook de grondreactiekrachten gemeten met een geïnstrumenteerde loopband. Gemeten grondreactiekrachten zijn vervolgens gebruikt als referentie om de schatting passend te maken aan de gemeten krachten en om het algoritme te valideren. Voor het passend maken van de schatting was een optimalisatiefunctie toegepast op het algoritme. Deze functie optimaliseert de kantelfrequenties van de filters, de filter orders en de wegingsfactor van de versnellingsdata van de sensoren door te zoeken naar de laagste kwadratisch gemiddelde afwijking (RMSE) tussen de schatting en de gemeten grondreactiekrachten. Door te optimaliseren voor de laagste RMSE, slaagde de optimalisatiefunctie erin zich te concentreren op de schatting van de totale loopcyclus. Hierdoor werden zowel de impactpiek als de actieve piek geschat. De laagste RMSE werd gevonden voor de bekken-tibia configuratie (0,129 BW). De bijbehorende kantelfrequenties, filter orders en wegingsfactor werden toegepast op de totale dataset en de absolute maximale actieve piekfout (AMAPE) en Pearsons correlatiecoëfficiënt (ρ) werden berekend. De AMAPE van de bekken-tibia configuratie was 0,0873 (± 0,0602) BW en de ρ was 0,99. De laagste AMAPE werd gevonden voor de bekken - dijen configuratie (0,0730 (± 0,0509) BW). Voor deze configuratie werd een RMSE van 0,180 BW en ρ van 0,98 gevonden. De pelvis - tibia configuratie is gevalideerd voor de drie loopsnelheden en drie stapfrequenties en er werd een sterke correlatie ($\rho > 0.99$) tussen de geschatte en gemeten grondreactiekrachten gevonden. Uit de gevoeligheidsanalyse bleek dat het voorgestelde algoritme goede schattingen kan maken bij kleine verschillen in de kantelfrequenties van de filters ten opzichte van de waarde die uit de optimalisatie volgde. Ook werd duidelijk dat andere filter ordes en wegingsfactor een hogere RMSE geven. Dit toont aan dat dat deze parameters nauwkeurig gekozen moeten worden. Kortom, het schatten van de verticale grondreactiekracht is mogelijk met drie sensoren, geplaatst op het bekken en beide tibia, en het voorgestelde algoritme. Hierbij wordt gebruik gemaakt van een tweede order filter met een kantelfrequentie van 7,4 Hz voor de pelvis, een vierde order filter met kantelfrequentie van 9,0 Hz voor de tibia en een wegingsfactor van 0,496 van de bekken versnelling.

ABSTRACT

Ground reaction forces (GRFs) are important measures to identify human movement. Someone standing, walking or running generates a force on the ground and as a reaction the GRF is applied on the body. The GRFs represent the load working on the body and are, therefore, often studied in running activities. This force may vary from 2 to 3 times body weight during running and is associated with running injuries. The GRF consists of three components of which the vertical force is the largest and most important component when studying injuries. The vertical GRF (vGRF) consists of first an impact peak and then an active peak. The first peak is generated by the impact the foot makes with ground and the second peak is a reaction of the neuromuscular feedback and push off force of the foot applied on the ground. GRFs can be measured using force plates mounted in the floor or instrumented in treadmills, however a restriction to this method is that is it limited to the lab setting. GRFs can also be estimated from other quantities. This could be used to determine the load on the body outside the lab. Different algorithms are developed for estimating GRFs based on inertial measurement units (IMUs), however no research has been done on estimating at different speed and step frequencies for rearfoot runners. The aim of this study is to develop a generic algorithm to estimate the vertical component of GRFs of rearfoot runners, using a minimal IMU setup.

Eight healthy experienced rearfoot strike runners (age: 33.75 ± 10.98 years; height: 1.77 ± 0.08 cm; mass: 70.46 ± 14.50 kg; gender: 5 males/ 3 females) participated in this study. Every participant ran at three different speeds (in random order 10, 12 and 14 km/h) and three different step frequencies (100%, 110% and 90% of preferred step frequency) for 90 seconds. IMU data of eight sensors was collected with the MVN Link system to be used for the estimation of the vGRFs. The estimation algorithm is based on Newtons second law and uses the accelerations of the sensors in global frame to estimate the vGRFs. Data of the instrumented treadmill was measured and used as a reference to fit and validate the algorithm. An optimization function was applied on the estimation algorithm to find the best fit to the measured GRF (mGRF). The function optimizes the filtering cutoff frequencies, the filtering orders and the weight factor (WF) of the accelerations of the sensors by searching for the lowest root mean squared error (RMSE). By optimizing for lowest RMSE, the optimization function managed to focus on the estimation of the total gait cycle. Hence, both the impact peak and active peak were estimated. The lowest RMSE was found for the pelvis - tibia configuration (0.129 BW). The corresponding cutoff frequencies, orders and WF were applied on the data set and the absolute maximum active peak error (AMAPE) and Pearson's correlation coefficient (ρ) were calculated. For the pelvis - tibia configuration an AMAPE of 0.0873 ($\pm$ 0.0602) BW and ρ of 0.99 was found. The lowest AMAPE was found for the pelvis - thighs configuration (0.0730 ($\pm$ 0.0509) BW). For this configuration a RMSE of 0.180 BW and ρ of 0.98 was found. The pelvis - tibia configuration is validated for the three running speeds and three step frequencies and strong correlation ($\rho > 0.99$) between the estimated and measured GRF was found. Sensitivity analysis showed that the proposed algorithm is able to estimate well for differences in cutoff frequencies of the filter and different participants. Small differences in filtering order and WF have quite a big influence on the RMSE and should be chosen precisely. In conclusion, estimation of the vGRF is possible using three sensors with the proposed estimation algorithm for the pelvis - tibia configuration. Sensor data should be filtered with a second order filter with pelvis f_c of 7.4 Hz, a fourth order filter with tibia f_c of 9.0 Hz and WF of 0.496 of the pelvis acceleration should be used.

SYMBOLS AND ACRONYMS

Symbol or Acronym	Definition	Unit
a	Acceleration	m/s^2
$a_{z,i}$	Acceleration of segment i in vertical direction	m/s^2
AMAPE	Absolute maximum active peak error	BW
BW	Body weight	
eGRF	Estimated ground reaction force	N
FSP	Foot strike pattern	
g	Gravitational acceleration	m/s^2
GRF	Ground reaction force	N
IMU	Inertial measurement unit	
m	Mass of a rigid body	kg
m_b	Body mass of the subject	kg
m_i	Body mass of segment i	kg
$MAP_{estimated}$	Estimated maximum active peak	BW
$MAP_{measured}$	Measured maximum active peak	BW
mGRF	Measured ground reaction force	N
N	Amount of segments	
RMSE	Root mean squared error	BW
vGRF	Vertical ground reaction force	N
$vGRF_{dynamic}$	Vertical ground reaction force of a dynamic body	N
$vGRF_{static}$	Vertical ground reaction force of a static body	N
WF	Weight factor	

CONTENTS

1 INTRODUCTION

Measuring ground reaction force (GRF) is of great interest in biomechanical analysis. This force represents an external whole-body biomechanical loading and is used to identify human movement (1). GRFs are forces applied on the body as a reaction of the forces exerted on the ground while standing, walking and running (2). Even though GRF is a reaction of the external loading, it is also influenced by muscular actions during activities and, therefore, affects the internal loads working on the different body parts as well (1). Since GRFs represent the loading on the body, it is often studied in running. During running this force can vary from 2- to 3-times body weight (BW) (3) and is, therefore, an indicator for running injuries (4). For this reason, it is important to measure and visualize the GRF during running activities.

GRFs are studied for different aspects, for example to determine musculoskeletal responses, for the evaluation of rehabilitation processes (5), to investigate gait patterns (6) and to examine injury-related factors (7). Different factors have an influence on the GRF, such as speed, step frequency and foot strike pattern (FSP). Higher speed is associated with higher GRF (8,9), whereas a higher step frequency will lead to a lower GRF (10,11). Besides that, every runner has their unique running technique, which can be classified by FSP. In general, three different FSP can be classified, namely, rearfoot strike (landing on the heel), midfoot strike (landing on the outside edge of the foot) and forefoot strike (landing on the forefoot) (12). The different FSPs lead to different muscle-tendon mechanics, leading to different GRF profiles (13), see Figure 1.

A.   **B.**   **C.**
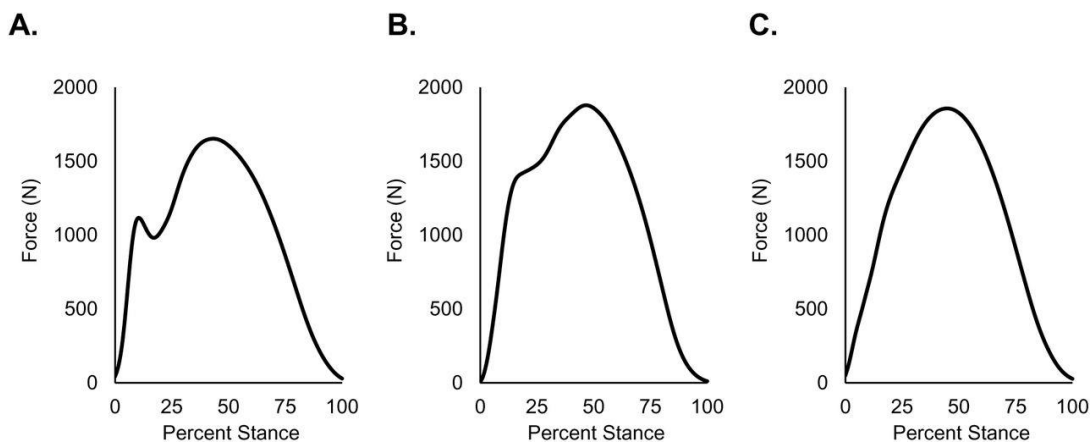
Figure 1: The vertical ground reaction force profiles for a rearfoot runner (A), midfoot runner (B) and a forefoot runner (C) (14)

For a rearfoot striker, the vertical component consists of two peaks, respectively the impact peak and the active peak (14,15). The first peak is generated by the impact the foot makes with ground. The second peak is a reaction of the neuromuscular feedback and push off force of the foot applied on the ground. Likewise, the vertical component of a midfoot striker consists of an impact peak and an active peak. However, for a midfoot and forefoot striker the presence of impact peak reduces, see Figure 1.

The GRF consists of three components, namely the mediolateral (the sideways force), the anterior-posterior (along the direction of motion) and the vertical (pointing upwards) component, defined as F_x, F_y and F_z respectively in this work, see also Figure 2. The vertical GRF is the biggest component and, therefore, this work will only focus on the vertical GRF.
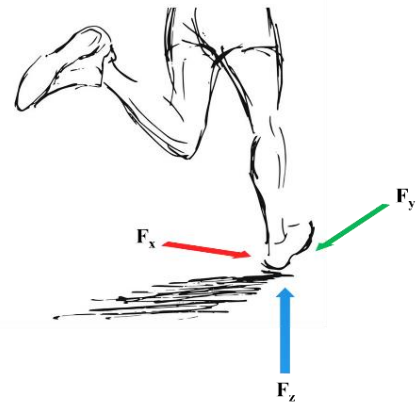
Figure 2: The components of the GRF

The GRF can be measured using force plates, which can either be mounted in the floor or instrumented in a treadmill. A drawback of this method is that it is restricted to the lab setting. However, GRFs can also potentially be estimated from other quantities. In the long run, this could mean that the load on the body can be determined in a sport-specific setting, outside the lab. Different algorithms are developed for estimating GRFs based on inertial measurement units (IMUs). An IMU consists of a three-axis gyroscope and a three-axis accelerometer to measure the angular velocities (deg/s^2) and linear accelerations (m/s^2) respectively (16). Some sensors also contain a magnetometer to measure the earth's magnetic field (8). By placing IMUs on the pelvis and lower legs, it is possible to estimate the vertical GRF (vGRF) for running using artificial neural networks (17). Neural networks are models that consist of mathematical equations connected to each other, where each mathematical equation stands for a biological process. Neural networks do have quite a lot of disadvantages, like being sensitive to overfitting and need great processing power (18). Therefore, neural networks are not preferable to use for real life applications. GRFs can also be estimated during mid stance in the single leg support phase for walking by taking the sum of the forces acting on the pelvis, upper legs and lower legs (19). These forces can be calculated by Newtons second law ($Force = mass \times acceleration$). For the terminal stance and double support phase, the GRFs was estimated using a cubic spline function. Despite being a valid method for four different step frequencies, this method assumes bilateral symmetry of the lower legs and is only validated in healthy subjects during walking (19). Comparably, the vGRF can be estimated with the sum of the forces of the pelvis and the upper legs using its kinematics and optimizing the values of the parameters to train the estimation model (20). This study obtained the kinematics by optical motion capture and performed grid-search to optimize the parameters.

An algorithm that estimates the vGRF using a minimal sensor setup could have the potential to analyze the human motion in real world scenarios, without being restricted to a lab. Previous research (17,19) has shown that it is possible to estimate GRFs based on IMUs, but no research has been done on estimating at different speed and step frequencies for rearfoot runners. This study only focused on estimating vGRF of rearfoot runners, since the impact peak is most present in the GRF profile and was expected to be the most difficult estimation. Therefore the **aim of this research** was to develop a generic algorithm to estimate the vertical GRFs of rearfoot runners, using a minimal IMU setup. The proposed algorithm is based on Newtons second law and, taking into account the factors that influence the GRF, will be evaluated for three running speeds and three different step frequencies, by comparing the estimated vGRF with the measured vGRF. It is expected that this algorithm will make good estimations of the vGRFs for rearfoot runners by using a maximum of three sensors at different speeds and step frequencies.

2 MATERIALS AND METHODS

2.1 Participants

Eight healthy experienced rearfoot strike runners (age: 33.75 ± 10.98 years; height: 1.77 ± 0.08 cm; mass: 70.46 ± 14.50 kg; gender: 5 males/ 3 females) participated in this study. Inclusion criteria included:

- running a minimum of 15 km/week for at least the past six months;
- an ability to run 14 km/h for 5 minutes straight;
- and not have had a major injury in the past six months.

Familiarity with treadmill running was favorable and participants being pregnant during the measurements were not included. All criteria were designed in such a way that the participants were able to complete the protocol without getting fatigued or injured. All participants read the information form and gave informed consent before the measurements. Participants were recruited via local (student) athletics and triathlon associations, using an (online) advertisement. All participants followed the same protocol, which was approved by the ethics committee (EEMCS) of the University of Twente as well as CCMO Arnhem/Nijmegen.

2.2 Materials

IMU data was collected using the MVN Link system (Xsens, Enschede, the Netherlands) with a sampling frequency of 240 Hz. The MVN Analyze software (Xsens, Enschede, the Netherlands) was used to record the data of the MVN Link system. Three dimensional GRFs were measured using a dual-belt instrumented treadmill (custom Y-mill, Motekforce Link, Culemborg, The Netherlands) with a sampling frequency of 2048 Hz. Video footages were collected with a high-speed camera (JVC GC-PX100BE) at 200 frames per second to confirm the participants' FSP. The step frequency was determined using an application (Tap BPM, suitable for android) on the mobile phone. A speaker was used to amplify the online metronome and to impose the high and low step frequency. MATLAB R2019a was used for the development and validation of the algorithm.

2.3 Sensor Placement and Measuring Body Dimensions

The full-body MVN Link system was converted into a lower body system (plus sternum) consisting of eight sensors. For other research purposes, an additional 'prop' sensor was placed on the distal side of the dominant tibia. The other eight sensors were placed on the trunk, pelvis, both upper legs, both proximal tibia and both feet, see Figure 3. All sensors were attached on the body using double sided tape. After placing the sensors, tape was used to fix the sensors to reduce motion artefacts. Glue spray was used only for the pelvis sensor, since participants were expected to sweat a lot on the lower back. Leg sleeves were put on the lower legs of the participants to decrease motion artifacts in the sensor data due to the impact created during running.
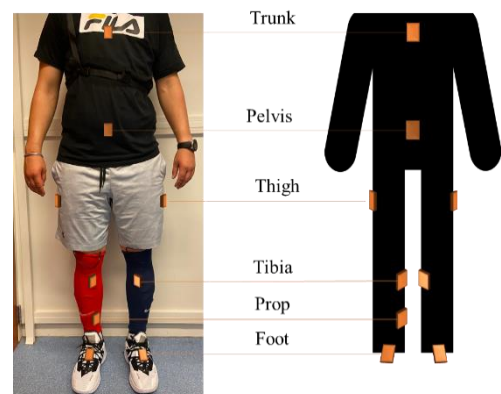
Figure 3: Sensor setup of the lower body system

Prior to the measurement, the body dimensions of the participants were measured. These included body height, shoe length, hip height, hip width, knee height and ankle height of the participant. These dimensions were necessary for the MVN Analyze software to correctly calibrate the lower body system.

2.4 Measurement Protocol

After measuring the body dimensions and placing the sensors, the system was calibrated following the protocol of the MVN Analyze software. This includes standing still in a steady upright neutral pose (N-pose) for 4 seconds, walking back and forth for about 8 steps and in the end standing still in starting position facing the starting direction. After four calibrations, the participants followed the measurement protocol which consisted of three different speeds (in random order 10, 12 and 14 km/h) and three different step frequencies (100%, 110% and 90% of preferred step frequency), see Figure 4 for a visual overview. First, the participant ran at the first speed with their preferred step frequency (100%) for 90 seconds. In the first 40 seconds of each trial, participants could accelerate and adjust to the step frequency of the metronome. The second 40 seconds of the first trial were used to measure the preferred step frequency using an application on the mobile phone. The high (110%) and low (90%) step frequency were then calculated based on the preferred step frequency. Then, the participant ran at high step frequency in the second and at low step frequency in the third trial of the same speed. After completing three trials of 90 seconds with three different step frequencies, the participant continued the same process for the second and third speed. There was a 3-minute rest period between trials in order to reduce the risk of the participant getting fatigued. Before and after each trial the participant jumped three times to synchronize the IMUs with the instrumented treadmill. After the measurement protocol, again four calibrations were performed.
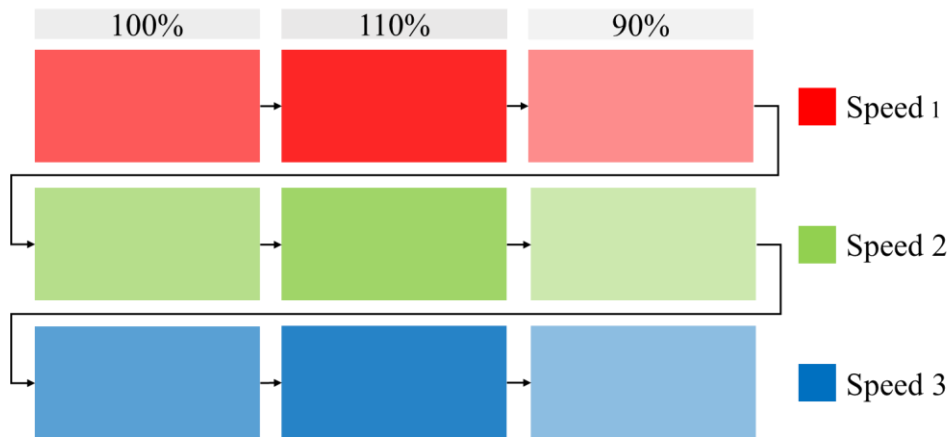
Figure 4: Graphic overview of the measurement protocol. Each trial lasted 90 seconds.

2.5 Data Collection

IMU data was collected with the MVN Link system using the MVN Analyze software. This software uses the participants' body dimensions (described in Section 2.3) to scale a biomechanical model to accurately track and estimate the motion of the participants (21). The mediolateral, anterior-posterior and vertical components of the free acceleration of the sensors in global frame were used for the estimation of the GRFs.

GRFs were measured with the instrumented treadmill in anterior-posterior, mediolateral and vertical directions during the measurement protocol. This measured GRF (mGRF) was used as a reference to fit (by optimizing) and validate the estimation algorithm. To determine the body weight of the participant, a measurement was performed in which the participant stood on the treadmill in the N-pose for at least 10 seconds.

Video footages of the participants' lower legs and feet were collected from a lateral view to identify their FSP. Participants were classified as a rearfoot strike runner if they first touched the treadmill with their heel when running at 10 km/h with their preferred step frequency. Participants were excluded if they were not a rearfoot strike runner.

The step frequency was determined during the preferred trial to calculate and impose the high and low step frequency. During the high and low trials, the step frequency was measured again to check the participants actual step frequency. Data was then categorized according to this measured step frequency. If the difference with the preferred step frequency was greater than 5%, the data was categorized to the high or low step frequency. If the difference with the preferred step frequency was less than 5%, the data was categorized to the preferred step frequency.

2.6 Data Processing

70 trials[1] in total (8 participants, 3 running speeds, 3 step frequencies) were processed in MATLAB. A frequency plot was made to determine the filtering options of the FP data. mGRFs data was filtered using a low-pass, eight-order, zero-phase shift Butterworth filter with a cutoff frequency (f_c) of 25 Hz. Acceleration data was up-sampled with the '*resample*' function in MATLAB to 2048 frames per second to match the sampling frequency of the treadmill. Afterwards, a cross-correlation function ('*xcorr*') was applied on the total data set to determine the lag between the acceleration data and the mGRF to synchronize both. For this, the sum of the right and left tibia accelerations was used. All accelerations were filtered using a low pass, zero-phase shift Butterworth filter to attenuate the signals with higher frequencies, i.e. noise and motion artefacts. The body mass was calculated in MATLAB by dividing the measured body weight by the gravitational acceleration ($9.81 \ m/s^2$).

2.7 Estimation

For the estimation of the GRF, the global free accelerations of the sensors of all subjects were used. Before doing the estimation, all sensor accelerations were analyzed by looking at the pattern of the acceleration against the stance phase percentage and comparing it with the mGRF. Possible sensor configurations were then determined. The sensor setup of all possible sensor configurations (from one to three sensors) can be found in 0. The estimation algorithm is described in Section 2.7.1. This algorithm was trained by optimizing the values of the parameters of the estimation algorithm. Optimization is further described in Section 2.7.2.

2.7.1 Estimation Algorithm

The algorithm to estimate the vGRFs is based on Newton's second law. According to Newton's second law the vGRF working on a stationary rigid body can be calculated with Equation 1:

$$vGRF_{static} = m \times g \tag{1}$$

with $vGRF_{static}$ the static vertical force (N), m the mass of the rigid body (kg) and g the gravitational acceleration (m/s^2). For a stationary human body consisting of N segments, the vertical GRF can be calculated by taking the sum of the segment forces following Equation 2:

$$vGRF_{static} = \sum_{i=1}^{N} m_i \times g \tag{2}$$

with m_i the body mass of segment i.

---

[1] Due to a problem in the left foot sensor, two trials are missing for one subject.

When the human body starts moving, i.e. walking or running, the segments start accelerating in different directions. To estimate the dynamic vGRF, the equation was rewritten as Equation 3:

$$vGRF_{dynamic} = (m_b \times g) + \sum_{i=1}^{N} m_i \times a_{z,i} \tag{3}$$

with m_b the total body mass of the subject, $a_{z,i}$ the vertical free acceleration of segment i and N the amount of segments. To determine the segment mass (m_i), a new variable, the weight factor (WF), was introduced. The WF is the percentage of the total body mass that contributes to the estimation, ranging from 0 - 1. Including the WF, Equation 3 can then be rewritten as:

$$vGRF_{dynamic} = (m_b \times g) + \sum_{i=1}^{N} m_b \times WF_i \times a_{z,i} \tag{4}$$

Only one segment (i) was included for the estimation with one sensor. The vGRF was, therefore, calculated by adding the body weight to the force acting on the location of the sensor. In conclusion, the estimation of the vGRF was achieved by Equation 5:

$$vGRF = m_b \times g + \left(m_b \times WF_1 \times acc_{sensor_1}\right) = m_b \left(\left(WF_1 \times acc_{sensor_1}\right) + g\right) \tag{5}$$

For the vGRF estimation with two symmetrically placed sensors, the lower body sensors were combined by adding them together. Both sensors were treated in the same way and, therefore, one weight factor was assigned. The estimation was done as following:

$$vGRF = m_b \left(\left(WF_1 \times \left(acc_{sensor_1} + acc_{sensor_2}\right)\right) + g\right) \tag{6}$$

Considering the estimation with three sensors, the lower body sensors ($sensor_2$ and $sensor_3$) were again added together. The first weight factor was assigned to the upper body sensor acceleration and the second weight factor was assigned to the lower body sensor acceleration. To equalize the equation, the second weight factor was multiplied with 0.5. The vertical GRF was then estimated with Equation 7:

$$vGRF = m_b \left(\left(WF_1 \times acc_{sensor_1}\right) + \left((0.5 \times WF_2) \times (acc_{sensor_2} + acc_{sensor_3})\right) + g\right) \tag{7}$$

with $sensor_1$ the trunk or pelvis sensor, $sensor_2$ and $sensor_3$ the thighs, tibia or feet sensors and WF_2 the weight factor of the left and right leg sensors. Since the weight acting on the body could not exceed the total body weight, WF_1 and WF_2 together equal one. Hence, Equation 7 was rewritten as following:

$$vGRF = m_b \left(\left(WF_1 \times acc_{sensor_1}\right) + \left((0.5 \times (1 - WF_1)) \times (acc_{sensor_2} + acc_{sensor_3})\right) + g\right) \tag{8}$$

2.7.2 Optimization

The discussed estimation algorithm is trained by optimizing the parameters, which are the filtering cutoff frequencies, filtering orders and the weight factors of the accelerations. An optimization function ('*fmincon*') is applied in MATLAB to find the most optimum values of the parameters by fitting the estimated GRF (eGRF) to the mGRF. This function starts the optimization at a given initial value for the

parameters and explores the values of these parameters to find the lowest value of a specified scalar equation. An additional option of this function is to set upper and lower boundaries for the optimized parameters. In this study, the scalar equation to be optimized was the root mean squared error (RMSE) between the eGRF and mGRF. RMSE is defined as:

$$RMSE = \sqrt{\sum_{i=1}^{n} \frac{(eGRF_i - mGRF_i)^2}{n}} \tag{8}$$

with n the number of data points. The optimization applied the values between the upper and lower boundaries and searched for the most optimal set of parameters with the minimum RMSE to fit the eGRF to the mGRF, see Figure 5 for a flow diagram for determining the parameters. For the estimation of the vGRF, the full data set consisting of the 70 trials measured of eight subjects was used. By selecting RMSE as optimization function, the eGRF will be optimized over the full stance phase. Hence, both the impact peak and active peak were estimated with lowest possible errors. The eGRF values lower than 20N were set to zero to prevent the algorithm from fitting non-stance phase values. This implies that the estimated values during the time between toe-off and the next heel strike (flight phase) were removed.

Optimized parameters were the cutoff frequencies, the orders of the filters and the weight factor of the sensor accelerations. The cutoff frequency was optimized for a broad range, namely 1 - 30 Hz for the upper body sensors and 1 - 15 Hz for the lower body sensors. The weight factor was optimized for a range of 0 - 1. The order of the filters were optimized for 2nd until 8th order with intervals of 2 orders.
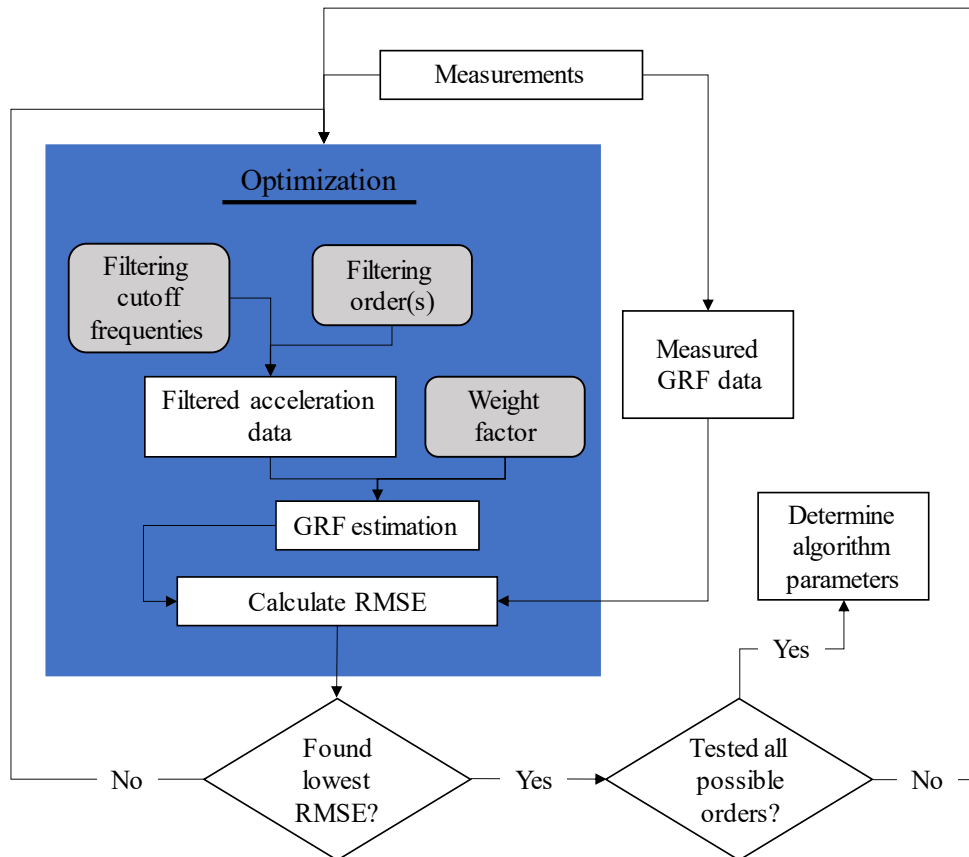
Figure 5: flow diagram showing the process starting from the measurements to determining the most optimal set of parameters. In grey, the optimized parameters are given. The optimization function searched for the most optimal set of parameters with the minimum RMSE between the eGRF to the mGRF by applying the values between the upper and lower boundaries of the parameters.

11

2.8 Outcome Measures

To evaluate the performance of the proposed algorithm, different measures were calculated and compared. The RMSE between the eGRF and mGRF was calculated while optimizing the algorithm. The optimization outcomes (cutoff frequencies, orders and weight factor) were applied on the full data set and analyzed. The maximum active peaks of the mGRF and eGRF were determined in MATLAB to calculate the absolute maximum active peak error (AMAPE), as given in Equation 9:

$$AMAPE = \left| \frac{MAP_{measured} - MAP_{estimated}}{(MAP_{measured})} \right| \times 100\% \tag{9}$$

with $MAP_{measured}$ the measured maximum active peak and $MAP_{estimated}$ the estimated maximum active peak. The AMAPE gives the accuracy of the algorithm for estimating the active peak of the vGRF. To test the correlation between the measured GRF and estimated GRF, the Pearson's correlation coefficient (ρ) was calculated in MATLAB. Leave-one-subject-out cross-validation was applied on the sensor configuration with the lowest RMSE to test the generalizability of the algorithm. The data of one subject was held aside to test the algorithm, where the remaining data of the other subjects was used to optimize the algorithm. This is repeated for every subject individually. Thus, eight different algorithms were developed and tested on all subject separately. Differences in the parameter values and the outcomes were analyzed.

2.9 Sensitivity Analysis

To test to what extent the RMSE is sensitive to changes in the optimized parameters, a sensitivity analysis was performed. To analyze how the RMSE is affected based on changes in the cutoff frequencies, a surface plot was made for the best sensor configuration. The RMSE values were calculated for different combinations of cutoff frequencies and were plotted against the cutoff frequencies in a three dimensional plot. Similarly, differences in the filter order and the weight factor were analyzed. To assess the generalizability of the algorithm for different running speeds and step frequencies, different categories of data sets have been analyzed. To test the generalizability of different speeds, data was categorized to either 10, 12 or 14 km/h. All categories included the preferred, high and low step frequency data of all subjects running at the speed of the category, see Table 1 for an overview of the included trials. In the same way, the step frequency data was categorized to preferred, high and low, see again Table 1. Each category was analyzed by calculating the RMSE, AMAPE and ρ for the best sensor configuration.

Table 1: Overview of the trials of all subjects that were included for the analysis of the different categories. The included trials can be found in the first column. For training the algorithm, the total data set was used (column 2). For analysis of each speed category (10, 12 and 14 km/h) included all trials of that same speed (column 3, 4 and 5 respectively). Each step frequency (preferred, high and low) included all trials of that same step frequency (column 6, 7 and 8 respectively).

Data set of trial	Full data set	10 km/h	12 km/h	14 km/h	Preferred	High	Low
10 km/h preferred	✓	✓			✓		
10 km/h high	✓	✓				✓	
10 km/h low	✓	✓					✓
12 km/h preferred	✓		✓		✓		
12 km/h high	✓		✓			✓	
12 km/h low	✓		✓				✓
14 km/h preferred	✓			✓	✓		
14 km/h high	✓			✓		✓	
14 km/h low	✓			✓			✓

3 RESULTS

3.1 Sensor Acceleration Analysis

Typical profiles of measured vGRF and the sensor accelerations can be found in Figure 6. In the upper left corner the mean stance phase of the gait cycle of the measured vGRF is presented in red. The impact peak is exerted until about 17% of the stance phase, where the active peak starts. In blue, the mean stance phase of the gait cycles of the right leg sensor accelerations in the z-axis is given. The trunk and pelvis accelerations both have a peak starting from about 17% and 20% respectively of the stance phase and therefore are useful for estimating the active peak. Both the tibia and foot accelerations have a clear peak between 0 and 20% of the stance phase, which could be useful for estimating the impact peak.
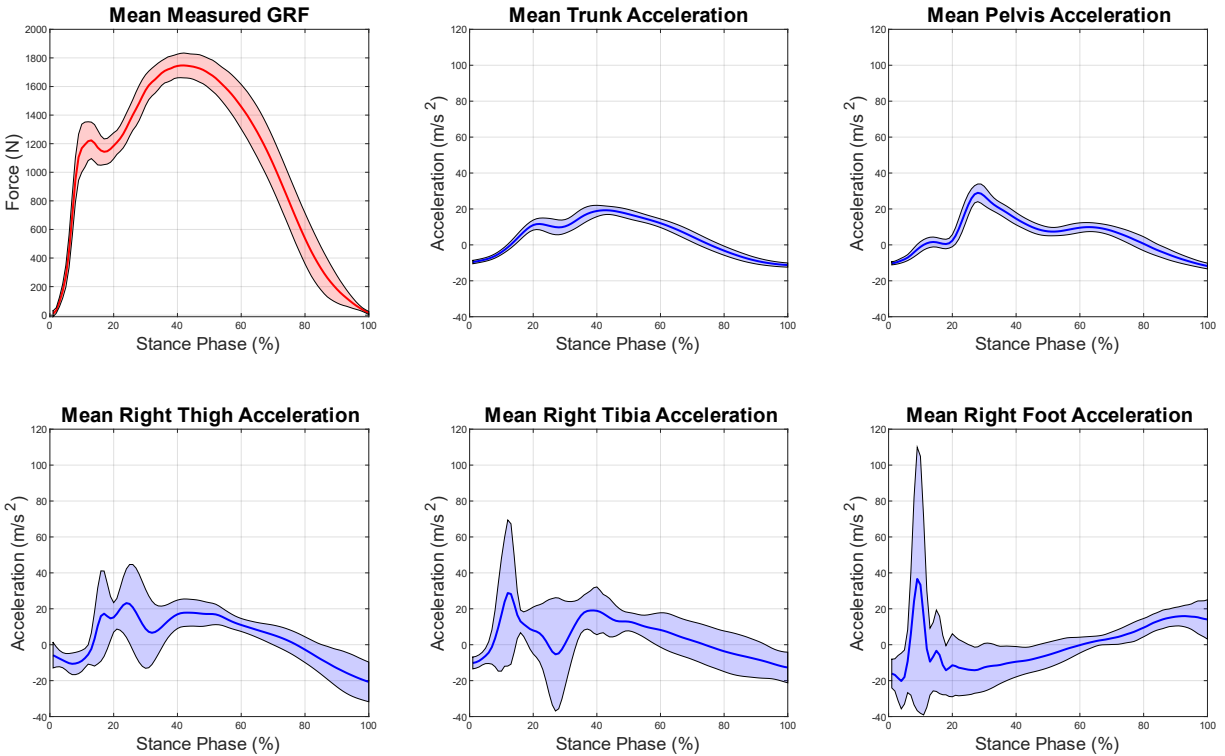
Figure 6: The mean gait cycle of the measured vGRF (in red) and the mean gait cycle of the sensor accelerations in the z-axis of the upper body and right leg sensors (in blue) over one stance phase of the gait cycle

To achieve the goal to develop an algorithm using a minimal IMU setup, a maximum of three sensors was used for the estimation. From the analysis of the sensor accelerations, estimating with three sensors seemed possible with combinations of one upper body and two lower body sensor accelerations. So, combinations could, for example, be the trunk accelerations with both thighs accelerations or the pelvis accelerations with both feet accelerations. When using lower body sensor accelerations, the sensor of the right side should always be combined with the identical sensor on the left side to obtain a full gait cycle. Therefore, combinations for the estimation with two sensors were both thighs, both tibia or both feet. While looking at the feet accelerations, it turned out that there was a problem with the left foot sensor. Therefore, the foot sensors were not further analyzed in this work. For the estimation using one sensor, the only possible two sensor configurations were the trunk or the pelvis accelerations. Estimation with three sensors was expected to have the best results, since both the impact peak and active peak would be estimated.

3.2 Vertical GRF Estimation

The outcomes of the optimized parameters (cutoff frequencies, orders of the filters and weight factor of the accelerations) and the accuracies (RMSE, AMAPE and ρ) of the estimated vGRF for all sensor configurations are presented in Table 2. Estimating the vGRF using three sensors had the best results, as expected from the analysis of the sensor accelerations. The sensor configuration consisting of the pelvis and both tibia sensors showed the lowest RMSE (0.13 BW). The pelvis acceleration was filtered with a fourth order lowpass filter with a cutoff frequency of 7.4 Hz and the tibia accelerations with a second order lowpass filter with a cutoff frequency of 9.0 Hz. The optimized weight factor of the pelvis accelerations equaled 0.496, whereas the weight factor of the right and left tibia accelerations together equaled 0.504. The lowest absolute maximum active peak error (0.0730 ± 0.0509 BW) was obtained by the pelvis - thighs configuration. Optimization outcomes were a cutoff frequency of 8.2 Hz for the pelvis accelerations, a cutoff frequency of 7.3 Hz for the thigh accelerations and a weight factor of 0.468 for the pelvis accelerations. A RMSE of 0.180 BW was found and was higher compared to the pelvis - tibia configuration. A strong correlation ($\rho > 0.97$) was found between the estimated GRF and measured GRF for all sensor configurations.

Table 2: The accuracy of the estimated vGRFs for all sensor configurations optimized for the total data set. The filtering cutoff frequencies (f_c), filtering orders and weight factor (WF) were determined by the optimization. Then, the root mean squared error (RMSE), absolute maximum active peak error (AMAPE) and Pearson's correlation coefficient (ρ) of the algorithm with the most optimum parameters were calculated.

Sensor Configuration	f_c (Hz)	Order	WF	RMSE (BW)	AMAPE $\pm$ std (BW)	%	ρ
Only trunk	5.7	6th	0.907	0.187	0.1160 ± 0.1110	4.76	0.98
Only pelvis	4.9	6th	0.929	0.194	0.0929 ± 0.0660	3.78	0.98
Both thighs	4.0	8th	0.954	0.224	0.0954 ± 0.0733	3.79	0.97
Both tibia	4.8	8th	1.000	0.221	0.1683 ± 0.1369	6.68	0.97
Trunk - thighs	7.6 - 4.0	6th - 4th	0.482	0.171	0.0895 ± 0.0802	3.67	0.98
Trunk - tibia	8.2 - 7.3	8th - 2nd	0.506	0.143	0.1566 ± 0.1064	6.36	0.99
Pelvis - thighs	6.1 - 4.1	6th - 4th	0.468	0.180	$\mathbf{0.0730 \pm 0.0509}$	**2.97**	0.98
Pelvis - tibia	7.4 - 9.0	4th - 2th	0.496	**0.129**	0.0873 ± 0.0602	3.54	0.99

The lowest RMSE is achieved with the pelvis - tibia configuration, whereas the lowest absolute maximum active peak is achieved with the pelvis - thighs configuration. In Figure 7, the mean stance phase with the standard deviation of the estimated vGRF are shown for both sensor configurations. On the left, the mean stance phase of the pelvis - thighs configuration and, on the right, the mean stance phase of the pelvis - tibia configuration are given. The pelvis - thighs configuration failed to estimate the impact peak, whereas the pelvis - tibia configuration succeeded in estimating the impact peak. Both configurations were able to estimate the active peak of the vGRFs. In Appendix - B:, the plots of the mean stance phases of all possible sensor configurations can be found.
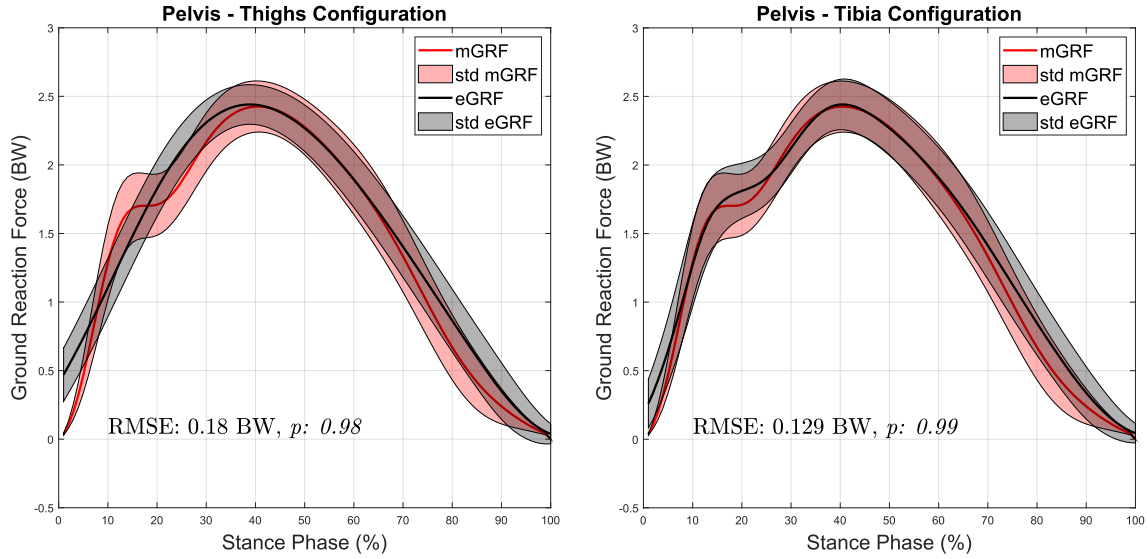
Figure 7: The mean stance phase and standard deviation of the gait cycle of the measured and the estimated vGRF determined for the total data set (for the pelvis - thighs configuration; on the left, and pelvis - tibia configuration; on the right), with the calculated root mean squared error (RMSE) and Pearson's correlation coefficient (ρ) between the eGRF and mGRF.

Since the pelvis - tibia configuration had the lowest RMSE (0.129 BW), a low AMAPE (0.0873 ± 0.0602 BW) and was able to estimate both the impact and active peak, this configuration was further analyzed. Leave-one-subject-out cross validation was applied to test the generalizability of the pelvis - tibia configuration. Each time, the data of one subject was excluded of the full data set and the parameters (pelvis f_c (Hz), tibia f_c (Hz) and WF) were optimized. In Table 3, the optimization outcomes are given for the data set that remained after excluding the subjects separately. For every data set, the optimization resulted in a fourth order lowpass filter for the pelvis and a second order lowpass filter for both tibia accelerations. Mean pelvis f_c of 7.5 ± 0.19 Hz, mean tibia f_c of 9.0 ± 0.16 Hz and mean WF of 0.496 ± 0.0078 of the pelvis acceleration is found. The cutoff frequencies of the accelerations and WF of the pelvis accelerations were close to the values of the optimized parameters of the full data set.

Table 3: The cutoff frequency (f_c) of the pelvis and tibia accelerations and the weight factor of the pelvis accelerations assessed using leave-one-subject-out cross-validation for the pelvis - tibia configuration with the lowest root mean squared error (RMSE; 0.129 BW).

Pelvis - Tibia	Excluded subject	Pelvis f_c (Hz)	Tibia f_c (Hz)	WF pelvis
	GIMUT 02	7.3	8.9	0.485
	GIMUT 04	7.5	9.1	0.497
	GIMUT 05	7.3	9.2	0.505
	GIMUT 07	7.7	9.0	0.482
	GIMUT 08	7.3	8.9	0.506
	GIMUT 09	7.2	8.7	0.504
	GIMUT 12	7.6	9.3	0.499
	GIMUT 13	7.8	9.2	0.490
	Full data set	7.4	9.0	0.496
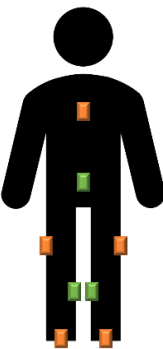
The optimization outcomes (pelvis f_c (Hz), tibia f_c (Hz) and WF) were applied on the excluded data set to test the accuracy of the algorithm. In Table 4, the results (RMSE, AMAPE and ρ) of the validation are given for each subject. A mean RMSE of 0.13 ± 0.015 BW and a mean AMAPE of 0.0889 ± 0.0286 BW was found. The results of the validation were close to the results of the estimation with the full data set. The estimated vGRF showed strong correlation ($\rho > 0.99$) with the measured vGRF for all validations.

Table 4: The optimization outcomes obtained by the leave-one-subject-out cross-validation applied on the subject that was left out and the calculated root mean squared error (RMSE), absolute maximum active peak error (AMAPE) and Pearson's correlation coefficient (ρ) between the estimated and measured GRF.

Subject	RMSE (BW)	AMAPE		ρ
		$\pm$ std (BW)	%	
GIMUT 02	0.1506	0.0656 $\pm$ 0.0489	2.41	0.99
GIMUT 04	0.1059	0.0589 $\pm$ 0.0454	2.58	0.99
GIMUT 05	0.1138	0.1092 $\pm$ 0.0676	4.28	0.99
GIMUT 07	0.1446	0.0874 $\pm$ 0.0580	3.69	0.99
GIMUT 08	0.1265	0.0722 $\pm$ 0.0486	3.09	0.99
GIMUT 09	0.1424	0.1305 $\pm$ 0.0520	5.05	0.99
GIMUT 12	0.1148	0.1373 $\pm$ 0.0646	5.74	0.99
GIMUT 13	0.1454	0.0503 $\pm$ 0.0375	2.05	0.99
Full data set	0.1294	0.0873 $\pm$ 0.0602	3.55	0.99

3.2.1 Sensitivity Analysis

A sensitivity analysis was performed to test the response of the RMSE to changes in the optimized parameters. First, the sensitivity of the filtering cutoff frequency was analyzed. The RMSE is calculated for different combinations of filtering cutoff frequencies of the pelvis and tibia accelerations and a surface plot was made, see Figure 8. The filtering orders and the weight factor of the pelvis and tibia accelerations were set to the value given Table 2. Between 8 - 10.5 Hz and 6.6 - 8.5 Hz, for the pelvis and tibia respectively, the RMSE is around 0.13 BW. The RMSE increases for higher cutoff frequencies.

To analyze the weight factor, all optimized parameters were fixed except for the weight factor. The RMSE was calculated for different weight factors ranging from zero to one and a plot was made, see Figure 10. The RMSE was lowest for about 0.5 weight factor of the pelvis acceleration and increases for higher and lower weight factors.
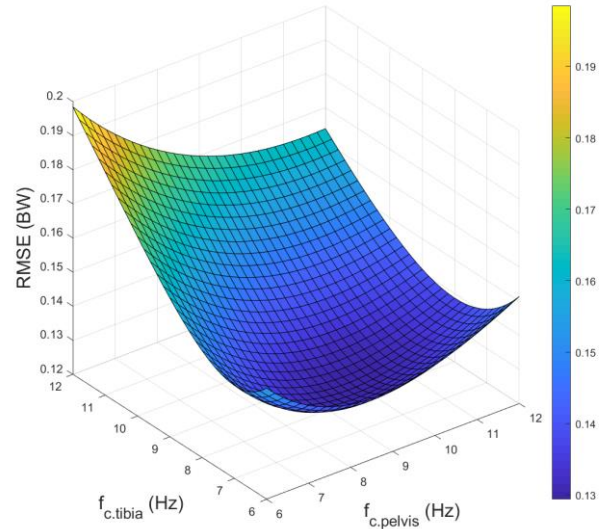
Figure 8: Surface plot with on the xy-plane the cutoff frequencies (f_c) of the pelvis and tibia accelerations and on the z-plane the root mean squared error (RMSE) of the pelvis - tibia configuration of the full data set.

The order of the filters were analyzed after fixing all parameter values except for the orders of the pelvis and tibia accelerations. The RMSE was then calculated for every possible combination of orders ranging from 2nd to 8th order, with intervals of 2 orders. In Figure 9, the surface plot is given with on the xy-plane the filtering orders and on the z-plane the RMSE. The lowest RMSE was found for a 4th order filter of the pelvis accelerations and 2nd order filter of the tibia accelerations. Different combinations of orders resulted in a quite higher RMSE.
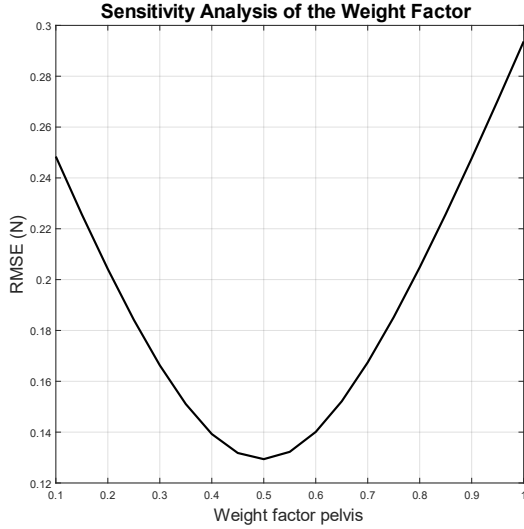
Figure 10: The root mean squared error (RMSE) against the weight factor (WF) for the analysis of the WF of the pelvis acceleration for the pelvis - tibia configuration.
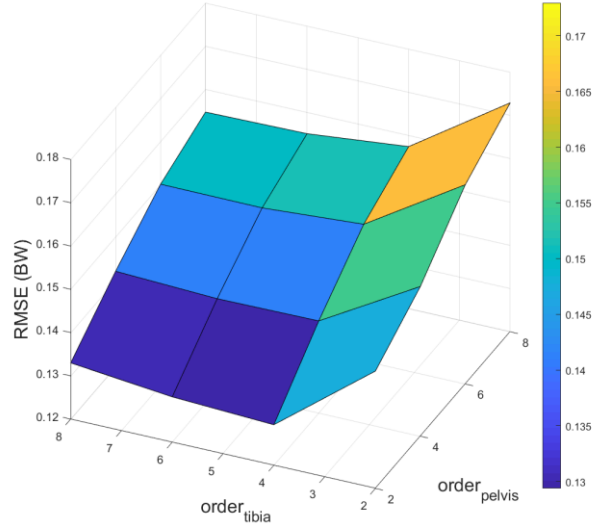
Figure 9: The surface plot for the filtering order analysis with on the xy-plane the order of the pelvis and tibia accelerations and on the z-plane the root mean squared error (RMSE) of the pelvis - tibia configuration.

3.2.2   Variation in Running Speed

To test the generalizability of the algorithm, the data was divided into the three speed categories (10, 12 or 14 km/h). The categorized speed data was then analyzed after applying the proposed estimation algorithm with the optimized parameters for the pelvis - tibia configuration. The accuracy of the algorithm for the different running speeds can be found in Table 5. The algorithm showed the best results for the lowest running speed (10 km/h), whereas the other running speeds showed higher errors. The higher the running speed, the higher the errors. The maximum active peak was estimated with small errors for all three speeds. The estimation showed strong correlation ($\rho > 0.99$) with the measured GRF for all running speeds.

Table 5: The root mean squared error (RMSE), absolute maximum active peak error (AMAPE) and Pearson's correlation coefficient (ρ) between the estimated and measured GRF calculated for the speed categoru, applied were the optimized parameters of the pelvis - tibia configuration.

Speed	RMSE (BW)	AMAPE		ρ
		$\pm$ std (BW)	%	
10 km/h	0.1150	0.0800 $\pm$ 0.0535	3.36	0.99
12 km/h	0.1269	0.0819 $\pm$ 0.0560	3.32	0.99
14 km/h	0.1445	0.0988 $\pm$ 0.0679	3.92	0.99
All speeds	0.1294	0.0873 $\pm$ 0.0602	3.55	0.99

In Figure 11, the mean (and standard deviation) vGRFs during the stance phase for the pelvis - tibia configuration are given for the three different speeds. The best estimation was obtained by the lowest running speed, 10 km/h. Small differences in GRF profiles were found between the different speeds. The highest speed had the highest active peak, whereas the lowest speed had the lowest active peak. In the same way, the impact peak was more present in the highest running speed. The same differences were found in the estimation of the vGRF.
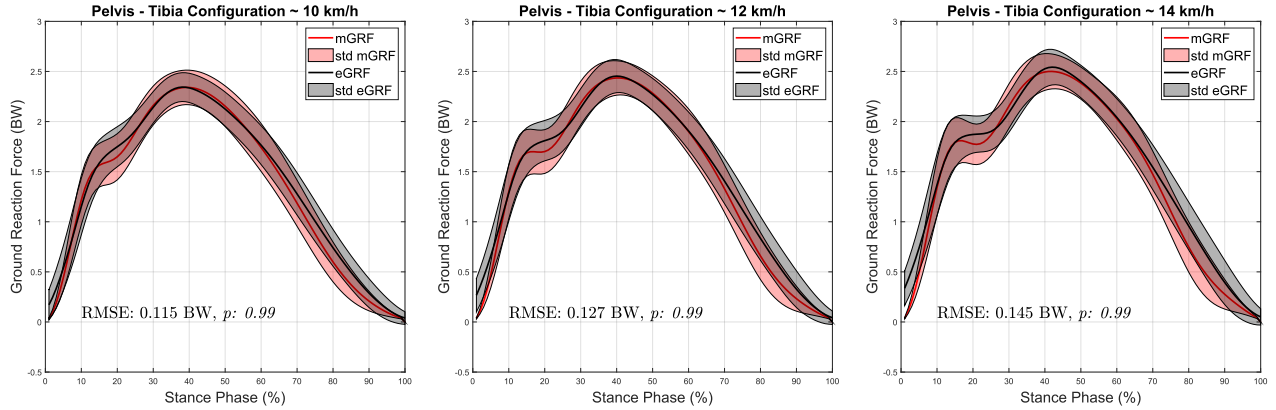
Figure 11: The mean measured and estimated vGRF against the stance phase for the different running speed data of the pelvis - tibia configuration. Given is also the root mean squared error (RMSE) and Pearson's correlation coefficient (ρ) between the estimated and measured vGRF.

3.2.3 Variation in Step Frequency

Similar to the speed analysis, the step frequency was analyzed to test the generalizability of the estimation algorithm. The data set was divided into three categories, namely preferred, high or low step frequency. Every category was analyzed for the pelvis - tibia configuration. In Table 6, the RMSE, AMAPE and ρ of the estimation can be found for the step frequency categories. High step frequency had the lowest error for whereas low step frequency had the highest error. Small differences were found between the categories for the AMAPE, but the highest error is again found for the low step frequency. All estimations showed strong correlation ($\rho > 0.99$) with the mGRF.

Table 6: The root mean squared error (RMSE), absolute maximum active peak error (AMAPE) and Pearson's correlation coefficient (ρ) between the estimated and measured GRF calculated for the step frequency data, applied were the optimized parameters for the total data set of the pelvis - tibia configuration.

Step Frequency	RMSE (BW)	AMAPE		ρ
		$\pm$ std (BW)	%	
Preferred	0.1294	0.0860 $\pm$ 0.0587	3.46	0.99
High	0.1248	0.0843 $\pm$ 0.0589	3.55	0.99
Low	0.1336	0.0912 $\pm$ 0.0629	3.61	0.99
All step frequencies	0.1294	0.0873 $\pm$ 0.0602	3.55	0.99

The mean (and standard deviation) stance phase of the vGRFs can be found for the three different step frequencies in Figure 12. Here, again differences in GRF profile were available between the categories. The active peak decreased when running at high step frequency, whereas the active peak increased when running at low step frequency. Compared to the preferred step frequency, the impact peak was more present for the low step frequency, while the impact peak was less present for the high step frequency. The same changes in GRF profile were found in the estimation of the different categories.
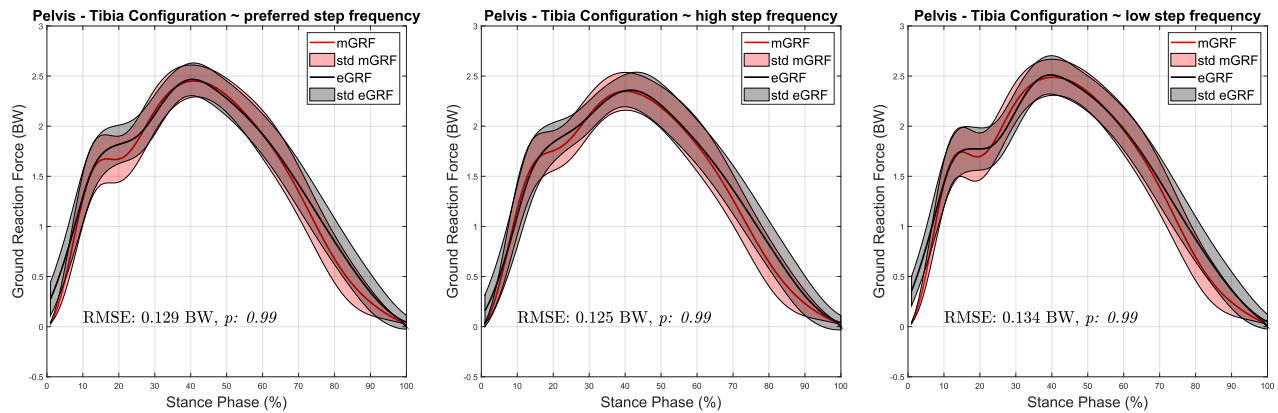
Figure 12: The mean estimated and measured vGRF and the standard deviation over the stance for the different step frequency data with the calculated root mean squared error (RMSE) and the Pearson's correlation coefficient (ρ) for the pelvis - tibia configuration.

4 DISCUSSION

The main goal of this research was to develop a generic algorithm to estimate vGRFs for rearfoot runners, using a minimal IMU setup. The results indicate that good estimation of the vGRF can be obtained for different running speeds and different step frequencies using three IMUs placed on the pelvis and both tibia.

Leave-one-subject-out cross-validation for the pelvis - tibia configuration resulted in small differences between the subjects. The cutoff frequencies of the accelerations were approximately the same as the cutoff frequency found by optimizing for the full data set. The same holds for the weight factor of the pelvis acceleration. This indicates that the results are generalizable and, therefore, the proposed algorithm and the optimized cutoff frequencies and weight factor of the pelvis acceleration would give good estimations when applied on runners beyond those studied in this research.

4.1 Implications

4.1.1 Theoretical Implications

Previous research showed that it is possible to estimate GRFs using IMUs by artificial neural networks and other mathematical calculations for example. For estimation of vGRFs with neural networks an RMSE < 0.27 BW was found (17). The algorithm proposed in this work finds a lower RMSE of 0.129 BW for the pelvis - tibia configuration.

Another study that partially estimated using Newton's second law and partially by a cubic spline function found a higher RMSE (19). An RMSE of 0.23 ($\pm$ 0.054) BW was found for walking at 60 steps per minute and an RMSE of 0.31 ($\pm$ 0.012) BW was found for walking at 120 steps per minute. This study, however, found a lower RMSE (0.129 BW) for running. This shows a good improvement of the estimation.

A comparable study used the accelerations obtained by optical motion capture and estimated the vGRFs for forefoot and rearfoot strikers using only Newton's second law (20). Grid-search was applied to find the best filtering cutoff frequency of the pelvis and thigh accelerations. An RMSE of 0.13 BW was found for estimation of all running speeds (2.5, 3.5 and 4.5 m/s). The proposed algorithm in this work finds an RMSE of 0.129 BW of the pelvis - tibia configuration. Thus, comparable performance was found. However, this work uses IMUs to obtain the pelvis and tibia acceleration and is, therefore, not restricted to a lab.

The results of the analysis of variation in step frequency support previous findings that a higher RMSE is found for estimations of higher step frequencies (19). Figure 12 shows that the estimation of the impact peak is worse for the high step frequency data compared to the low step frequency data. It is shown that the impact shock attenuation increases with step frequency (22) and, thus, the impact peak accelerations decrease for higher step frequencies. Consequently, the RMSE is higher due to the fact that the impact peak is not estimated precisely.

Acceleration data was collected with a sampling frequency of 240 Hz, whereas mGRF was collected with a sampling frequency of 2048 Hz. The acceleration data was up-sampled to 2048 Hz to equalize the sampling frequency. A drawback of resampling is that data points are obtained by interpolation. Despite, the errors between the estimation and mGRF are quite low.

The figures of the mean stance phase of the gait cycle show that the mGRF profile differs for different speed and different step frequency. It can also be seen that the estimation follows these differences in the mGRF, which concludes that the algorithm is able to estimate vGRF for these factors with low errors.

4.1.2 Practical Implications

Current methods to determine GRFs are restricted to the lab setting. This study, however, shows that the vGRF can be estimated using three IMUs mounted on the runners body. This means that the vertical load on the body can be determined outside the lab. Eventually, the human motion can be analyzed. Thus, the estimation algorithm with the pelvis - sensor configuration proposed in this work is a step forward in the direction of a GRF monitoring system for runners in the sport-specific setting.

The proposed algorithm uses the sensor free acceleration in global frame for the estimation of vGRFs. An advantage of using accelerations in the global frame is that this approach could estimate the GRFs regardless of the location on earth. However, a magnetometer is required to measure in or to rotate to the global frame. This holds that the proposed estimation algorithm is not applicable for sensors only containing an accelerometer (and gyroscope).

During the measurements, glue spray is used to fix the pelvis sensor and prevent motion artefacts, since runners do sweat a lot on the pelvis. Nevertheless, some participants still indicated that the pelvis sensor got loose during the measurement. For everyday use while running, runners should attach the sensor properly by using straps or pull their running shorts over the sensor for example. To prevent movement of the tibia sensors, leg sleeves were used on the lower legs. In daily life, runners should also make use of leg sleeves or compression socks to achieve good estimation.

4.2 Limitations and Further Research

This section discusses the limitations and possible improvements that can be made to further develop the proposed algorithm. To start with, only eight participants were included in this study. The optimization should be performed with more subjects in order to reduce the risk of bias as well as to increase the generalization of the proposed algorithm.

Besides, body dimensions vary from person to person, leading to different segment mass ratios. One has, for example, heavier lower legs compared to their upper body, whereas someone else has a heavier upper body compared to their lower body. To avoid ratios playing a role, it is important to include multiple different participants and revalidate the algorithm in order to get the most optimum weight factor. AWF of 0.496 for the pelvis acceleration and 0.252 for each tibia was found in this work. In previous research, a segment weight of 0.161 BW of the total leg was found (23). The upper body weight was then 0.678 of the total body weight. These values are clearly different than the WF found in this research. The reason for this is that the WF in this research is optimized together with the cutoff frequency and the order of the filters. The WF does represent the amount in which the accelerations contribute to the estimations and not directly the segment masses of the subjects.

Another limitation concerns the protocol and inclusion criteria of the measurements. The protocol and inclusion criteria aimed to reduce the risk of participants from getting fatigued. Additional research could be conducted to evaluate the accuracy of the estimation on fatigued runners. Besides, only experienced rearfoot strike runners were included in this study. As mentioned in the Introduction, different FSP result in different vGRF profiles. This algorithm is validated for only rearfoot runners and should be tested for different foot strike patterns by applying the optimization parameters of the pelvis - tibia configuration and validating for midfoot and forefoot runners. Similarly, the proposed method could be validated for unexperienced runners.

For the analysis of variation in running speed and step frequency the validated data set was also used for training the algorithm. From this, it could not be concluded whether the algorithm generalizes well to other running speeds and step frequencies. The validation should, therefore, be performed on new data containing different speeds and step frequencies than the ones studies in this research.

Due to missing foot accelerations and an error in the foot sensor, this sensor was not further analyzed in this work. However, to measure accelerations and also the external mechanical load on the body, IMUs can also be placed on the feet (24). Foot acceleration may be an improvement on the proposed algorithm and, therefore, further research is needed to establish the validity of configurations including the foot sensors.

As discussed in Section 4.1.2, the proposed algorithm is not able to estimate the vGRFs using accelerations measured in the sensor frame. To rotate from sensor frame to the global frame, in which the algorithm works, a magnetometer is necessary. However, the vGRF in global frame is in the same direction as the vGRF in the body frame. The vertical axis of the body frame can be determined by adding a calibration consisting of one rotational movement around the vertical axis (z-axis). For this, a gyroscope is needed to detect the rotations. During the (running) activity, the gyroscope will detect the rotations of the sensors in z-axis. By applying this in the algorithm, accelerations in sensor frame can be rotated to a world fixed body frame to estimate the vGRFs.

As shown in Table 2, the WF for the estimation with the trunk, pelvis and both thighs configuration is not equal to 1. This means that the total body mass of the participant is not used for the estimation. The proposed algorithm in this work, however, assumed that the total body mass is needed for the three sensors configuration. Hence, further research could introduce a WF factor and optimize it to check whether the total body mass is indeed required for the estimation.

5   CONCLUSION

In this work, an algorithm is developed to estimate vGRFs during running activities. This algorithm is validated for different sensor configurations and best performance is obtained for the pelvis - tibia configuration. This configuration consists of three sensors placed on the pelvis and on both tibia. For this configuration, an RMSE of 0.129 BW and an AMAPE of 0.0873 ($\pm$ 0.0602) BW is found. Compared to other studies, a lower RMSE is obtained. Validating for the different running speeds and step frequencies for RMSE and AMAPE shows that the algorithm has a good potential to estimate vGRFs. Sensitivity analysis shows that small differences in cutoff frequencies and for different subjects the proposed method is still promising. Filtering order and WF, however, should be chosen properly in order to obtain the lowest errors between the eGRF and mGRF. In conclusion, the pelvis - tibia configuration gives the lowest RMSE for the proposed estimation algorithm, using a second order filter with pelvis f_c of 7.4 Hz, a fourth order filter with tibia f_c of 9.0 Hz and WF of 0.496 of the pelvis acceleration.

6   ACKNOWLEDGEMENTS

REFERENCES

1.   Verheul J. Biomechanical loads in running-based sports: Estimating ground reaction forces from segmental accelerations (PhD Academy Award) [Internet]. Vol. 54, British Journal of Sports Medicine. BMJ Publishing Group; 2020 [cited 2021 Jun 19]. Available from: https://bjsm.bmj.com/content/54/14/879

2.   Charry E, Hu W, Umer M, Ronchi A, Taylor S. Study on estimation of peak Ground Reaction Forces using tibial accelerations in running. In: Proceedings of the 2013 IEEE 8th International Conference on Intelligent Sensors, Sensor Networks and Information Processing: Sensing the Future, ISSNIP 2013. 2013. p. 288–93.

3.   Lieberman DE, Venkadesan M, Werbel WA, Daoud AI, D'Andrea S, Davis IS, et al. Foot strike patterns and collision forces in habitually barefoot versus shod runners. Nat 2010 4637280 [Internet]. 2010 Jan 27 [cited 2021 Aug 17];463(7280):531–5. Available from: https://www-nature-com.ezproxy2.utwente.nl/articles/nature08723

4.   Bonacci J, Saunders PU, Hicks A, Rantalainen T, Vicenzino B (Guglielmo) T, Spratford W. Running in a minimalist and lightweight shoe is not the same as running barefoot: a biomechanical study. Br J Sports Med [Internet]. 2013 Apr 1 [cited 2021 Aug 17];47(6):387–92. Available from: https://bjsm.bmj.com/content/47/6/387

5.   Chmielewski TL, Myer GD, Kauffman D, Tillman SM. Plyometric exercise in the rehabilitation of athletes: Physiological responses and clinical application [Internet]. Vol. 36, Journal of Orthopaedic and Sports Physical Therapy. Movement Science Media; 2006 [cited 2021 Jul 2]. p. 308–19. Available from: https://pubmed-ncbi-nlm-nih-gov.ezproxy2.utwente.nl/16715831/

6.   Vaverka F, Elfmark M, Svoboda Z, Janura M. System of gait analysis based on ground reaction force assessment. Acta Gymnica [Internet]. 2015 Dec 31 [cited 2021 Jul 2];45(4):187–93. Available from: http://gymnica.upol.cz/doi/10.5507/ag.2015.022.html

7.   Bates NA, Ford KR, Myer GD, Hewett TE. Impact differences in ground reaction force and center of mass between the first and second landing phases of a drop vertical jump and their implications for injury risk assessment. J Biomech. 2013 Apr 26;46(7):1237–41.

8.   Kyröläinen H, Belli A, Komi P V. Biomechanical factors affecting running economy. Med Sci Sports Exerc [Internet]. 2001 [cited 2020 Sep 24];33(8):1330–7. Available from: https://pubmed.ncbi.nlm.nih.gov/11474335/

9.   Wang X, Ma Y, Hou BY, Lam WK. Influence of Gait Speeds on Contact Forces of Lower Limbs. J Healthc Eng [Internet]. 2017 [cited 2020 Sep 24];2017. Available from: https://pubmed.ncbi.nlm.nih.gov/29065630/

10.   Morin JB, Samozino P, Zameziati K, Belli A. Effects of altered stride frequency and contact time on leg-spring behavior in human running. J Biomech. 2007 Jan 1;40(15):3341–8.

11.   Heiderscheit BC, Chumanov ES, Michalski MP, Wille CM, Ryan MB. Effects of step rate manipulation on joint mechanics during running. Med Sci Sports Exerc [Internet]. 2011 Feb [cited 2021 Mar 17];43(2):296–302. Available from: /pmc/articles/PMC3022995/

12.   Hoenig T, Rolvien T, Hollander K. Footstrike patterns in runners: Concepts, classifications, techniques, and implications for running-related injuries. Dtsch Z Sportmed. 2020 Mar 1;71(3):55–61.

13.   Yong JR, Dembia CL, Silder A, Jackson RW, Fredericson M, Delp SL. Foot strike pattern during running alters muscle-tendon dynamics of the gastrocnemius and the soleus. Sci Rep [Internet]. 2020

Dec 1 [cited 2020 Nov 3];10(1). Available from: /pmc/articles/PMC7125118/?report=abstract

14.   Zadpoor AA, Nikooyan AA. The effects of lower-extremity muscle fatigue on the vertical ground reaction force: A meta-analysis [Internet]. Vol. 226, Proceedings of the Institution of Mechanical Engineers, Part H: Journal of Engineering in Medicine. SAGE PublicationsSage UK: London, England; 2012 [cited 2021 Jul 5]. p. 579–88. Available from: https://journals.sagepub.com/doi/10.1177/0954411912447021?url_ver=Z39.88-2003&rfr_id=ori%3Arid%3Acrossref.org&rfr_dat=cr_pub++0pubmed

15.   Kleiner AFR, Carmo AA do, Kletecke R, Burgos D, Souza MF de, Barros RML de. Ground reaction forces analyses during the gait of healthy individuals with and without the use of a calcaneus insole. Acta Fisiátrica. 2012;19(1):1–5.

16.   Zhou L, Fischer E, Tunca C, Brahms CM, Ersoy C, Granacher U, et al. How We Found Our IMU: Guidelines to IMU Selection and a Comparison of Seven IMUs for Pervasive Healthcare Applications. Sensors (Basel) [Internet]. 2020 Aug 1 [cited 2021 Nov 1];20(15):1–28. Available from: /pmc/articles/PMC7435687/

17.   Wouda FJ, Giuberti M, Bellusci G, Maartens E, Reenalda J, van Beijnum BJF, et al. Estimation of vertical ground reaction forces and sagittal knee kinematics during running using three inertial sensors. Front Physiol [Internet]. 2018 Mar 22 [cited 2021 Jul 4];9(MAR):218. Available from: www.frontiersin.org

18.   Tu J V. Advantages and disadvantages of using artificial neural networks versus logistic regression for predicting medical outcomes. J Clin Epidemiol. 1996 Nov 1;49(11):1225–31.

19.   Ohtaki Y, Sagawa K, Inooka H. A method for gait analysis in a daily living environment by body-mounted instruments. JSME Int Journal, Ser C Mech Syst Mach Elem Manuf. 2001 Dec;44(4):1125–32.

20.   Komaris DS, Perez-Valero E, Jordan L, Barton J, Hennessy L, O'Flynn B, et al. Effects of segment masses and cut-off frequencies on the estimation of vertical ground reaction forces in running. J Biomech. 2020 Jan 23;99:109552.

21.   Schepers M, Giuberti M, Bellusci G. Xsens MVN: Consistent Tracking of Human Motion Using Inertial Sensing. 2018.

22.   Hamill J, Derrick TR, Holt KG. Shock attenuation and stride frequency during running. Hum Mov Sci. 1995 Jun 1;14(1):45–60.

23.   Anthropometry [Internet]. Biomechanics and Motor Control of Human Movement. 2009. p. 82–106. (Wiley Online Books). Available from: https://doi.org/10.1002/9780470549148.ch4

24.   Glassbrook DJ, Fuller JT, Alderson JA, Doyle TLA. Foot accelerations are larger than tibia accelerations during sprinting when measured with inertial measurement units. J Sports Sci [Internet]. 2020 Feb 1 [cited 2021 Oct 1];38(3):248–55. Available from: https://www.tandfonline.com/action/journalInformation?journalCode=rjsp20

APPENDIX

Appendix - A: Sensor Configurations

All possible sensor configurations with combinations of one sensor up to three sensors, with in green the included sensor(s).
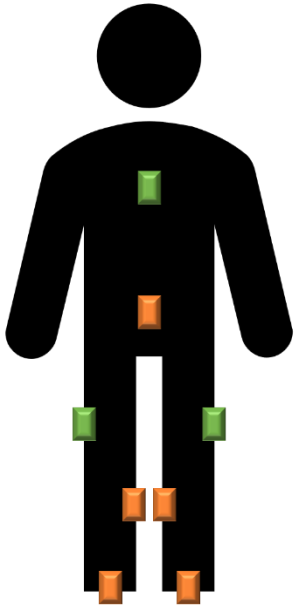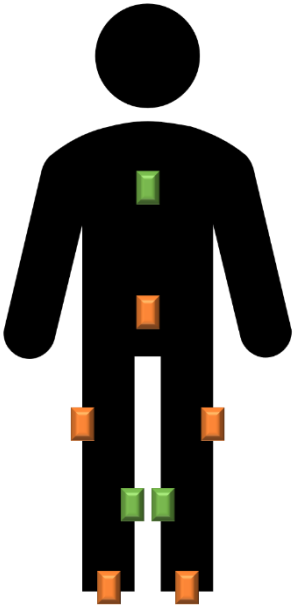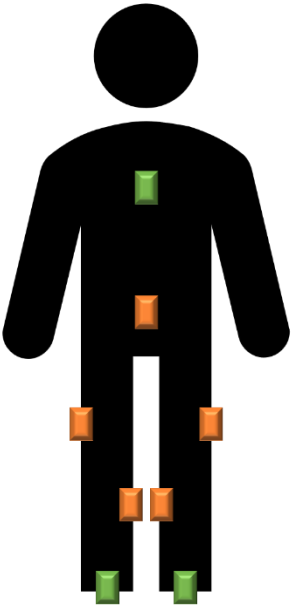
3 sensors		
Trunk - thighs	Trunk - tibia	Trunk - feet
3 sensors		
Pelvis - thighs	Pelvis - tibia	Pelvis - feet
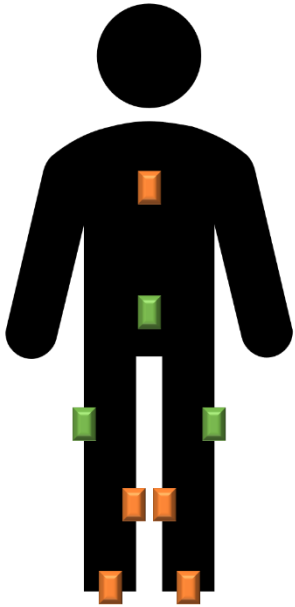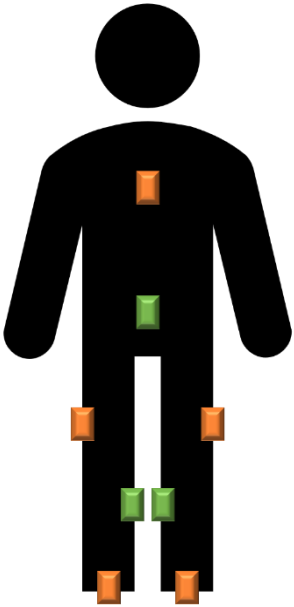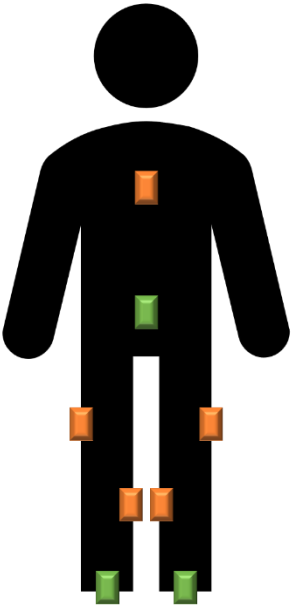
Appendix - B: Mean stance phases of all tested sensor configurations

The mean and standard deviation of the vGRFs during the stance phase for all the tested sensor configurations of one to three sensors.

Trunk - thighs

Trunk - tibia

Pelvis - thighs

Pelvis - tibia